# Inhibitors of GLUT/SLC2A Enhance the Action of BCNU and Temozolomide against High-Grade Gliomas

Alberto Azzalin[*,†], Giulia Nato[‡], Elena Parmigiani[‡], Francesca Garello[§], Annalisa Buffo[‡] and Lorenzo Magrassi[*,†]

*Neurochirurgia, Dipartimento di Scienze Clinico-Chirurgiche, Diagnostiche e Pediatriche, University of Pavia - Fondazione IRCCS Policlinico S. Matteo, v.le Golgi 19, 27100 Pavia, Italy; †Istituto di Genetica Molecolare IGM-CNR, via Abbiategrasso 207, 27100 Pavia, Italy; ‡Department of Neuroscience Rita Levi-Montalcini, University of Turin, Neuroscience Institute Cavalieri Ottolenghi (NICO), 10043 Orbassano, (Torino), Italy; §Molecular & Preclinical Imaging Centers, Department of Molecular Biotechnology and Health Sciences, University of Torino, Via Nizza 52, 10126 Torino, Italy

## Abstract

Glucose transport across glioblastoma membranes plays a crucial role in maintaining the enhanced glycolysis typical of high-grade gliomas and glioblastoma. We tested the ability of two inhibitors of the glucose transporters GLUT/SLC2A superfamily, indinavir (IDV) and ritonavir (RTV), and of one inhibitor of the Na/glucose antiporter type 2 (SGLT2/SLC5A2) superfamily, phlorizin (PHZ), in decreasing glucose consumption and cell proliferation of human and murine glioblastoma cells. We found *in vitro* that RTV, active on at least three different GLUT/SLC2A transporters, was more effective than IDV, a specific inhibitor of GLUT4/SLC2A4, both in decreasing glucose consumption and lactate production and in inhibiting growth of U87MG and Hu197 human glioblastoma cell lines and primary cultures of human glioblastoma. PHZ was inactive on the same cells. Similar results were obtained when cells were grown in adherence or as 3D multicellular tumor spheroids. RTV treatment but not IDV treatment induced AMP-activated protein kinase (AMPKα) phosphorylation that paralleled the decrease in glycolytic activity and cell growth. IDV, but not RTV, induced an increase in GLUT1/SLC2A1 whose activity could compensate for the inhibition of GLUT4/SLC2A4 by IDV. RTV and IDV pass poorly the blood brain barrier and are unlikely to reach sufficient liquoral concentrations *in vivo* to inhibit glioblastoma growth as single agents. Isobologram analysis of the association of RTV or IDV and 1,3-bis(2-chloroethyl)-1-nitrosourea (BCNU) or 4-methyl-5-oxo-2,3,4,6,8-pentazabicyclo[4.3.0]nona-2,7,9-triene-9-carboxamide (TMZ) indicated synergy only with RTV on inhibition of glioblastoma cells. Finally, we tested *in vivo* the combination of RTV and BCNU on established GL261 tumors. This drug combination increased the overall survival and allowed a five-fold reduction in the dose of BCNU.

*Neoplasia (2017) 19, 364–373*

## Introduction

The prognosis of glioblastoma multiforme (GBM) remains poor with a median survival of approximately 15 months [1]. The standard of care for GBM comprises aggressive neurosurgery aiming at complete macroscopic tumor resection, radiotherapy, and chemotherapy. Alkylating agents like 1,3-bis(2-chloroethyl)-1-nitrosourea (BCNU) and 4-methyl-5-oxo-2,3,4,6,8-pentazabicyclo[4.3.0]nona-2,7,9-triene-9-carboxamide (TMZ) are the only chemotherapeutic agents

that have been demonstrated active against GBM in large prospective trials. Despite its longer history, BCNU has been largely supplanted by TMZ due to easiness of administration (e.v. versus oral) and a lower level of long-term nonhematologic toxicity compared with nitrosureas [2]. The total cumulative dose of BCNU predicts the risk of inducing severe pulmonary fibrosis and delayed hepatotoxicity [3–5], thus limiting dose escalation. Despite a similar mechanism of action, BCNU and TMZ may have a modest synergistic inhibitory effect on glioma growth [6,7]. Moreover, resistance to TMZ treatment does not necessarily imply resistance to BCNU both *in vitro* and *in vivo* [8,9]. These facts generated a renewed interest in BCNU for recurrent GBM treatment after TMZ chemotherapy, a clinical setting where no validated treatments are available [10]. To improve the therapeutic potential of BCNU and TMZ against GBM, we studied if the synchronous administration of drugs blocking glucose entry into GBM cells resulting in a reduction of the aerobic glycolysis could potentiate the effects of the two agents. Glucose transport into glioblastoma cells depends mainly on glucose transporters of the GLUT/SLC2A superfamily [11–13], but other endo and exo transporters have also been detected in glioblastoma [14]. Both the Na/glucose antiporter type 2 (SGLT2/SLC5A2) and HsSWEET1 (SLC50A1), the only human protein member of the "Sugar Will Eventually be Exported Transporter" (SWEET) superfamily, were found in glioblastoma cells [14]. Ketogenic diets where carbohydrates are substituted by fats are potentially useful to reduce the glycolytic metabolism of glioblastoma through a reduction of glucose entrance in glioblastoma cells and other effects on glycolysis [15]. However, the clinical studies available so far indicate that this approach has only a minor effect on tumor growth and only when it is adopted in combination with other therapies [16]. Pharmacologic inhibition of activity of some members of GLUT/SLC2A can be obtained *in vitro* and *in vivo* by treatment with IDV and RTV originally developed as inhibitors of HIV-1 protease [17]. IDV is specific for GLUT4/SLC2A4, whereas RTV is active, albeit at different levels, against GLUT1/SLC2A1, GLUT3/SLC2A3, and GLUT4/SLC2A4 [18,19]. In this study, we investigated the effects of IDV, RTV, and PHZ, an inhibitor of SGLT1 and SGLT2, on human and murine glioblastoma cells. We also studied the activity of these drugs on glioblastoma cells in combination with BCNU or TMZ. Because we found that RTV and BCNU have the best synergic effect *in vitro*, we tested their activity *in vivo* against tumors obtained by inoculating murine glioblastoma cells from the GL261 cell line [20] in the brain of mice. Our study demonstrates that the addition of RTV to BCNU potentiates the effect of BCNU, reaching therapeutic efficacy at doses well below the standard recommended for BCNU alone.

## Materials and Methods

### Cell Lines and Culture

We used two stable human glioblastoma cell lines, U87MG [21,22] and Hu197 [23], and one primary human glioblastoma cell culture, GBM-P1, obtained from a human glioblastoma sample [24] and frozen after brief stabilization and expansion *in vitro* in serum-free conditions. GBM-P1 cells were tested after less than four passages *in vitro*. We also used *in vitro* and *in vivo* cells from a mouse glioblastoma cell line, GL261 [20], and a stable GL261 clone expressing the enhanced version of the green fluorescent protein (eGFP) under the immediate-early human cytomegalovirus promoter

selected after retroviral infection of the parental cell line. U87MG cells were maintained in adherent cultures or as multicellular spheroids in E-MEM medium supplemented with 10% FBS, 100 U/ml of penicillin, 0.1 mg/ml of streptomycin, and 8 μg/ml of ciprofloxacin at 37°C and 5% CO2 atmosphere; all other stable cell lines were cultivated in D-MEM medium supplemented with 10% FBS, 100 U/ml of penicillin, 0.1 mg/ml of streptomycin, 2 mM L-glutamine, and 8 μg/ml of ciprofloxacin. Primary cultures were maintained as previously described [24]. Spheroid formation was induced by plating the cells over standard microbiology tissue culture petri dishes [24] and maintained as described for the adherent cultures. Spheroids diameter varied from about 10 to 100 μm. All cell culture reagents were purchased from Euroclone (Milan, Italy) except for E-MEM (ATCC, Teddington, Middlesex, UK).

Microphotographs were obtained through an inverted microscope (Leica Microsystems, Milan, Italy) equipped with phase contrast and dark field illumination. All microphotographs were taken through a digital camera (Canon) and the associated "Canon Utilities Remote Capture" (Version 2.6.0.10).

### Chemical Reagents and Antibodies

Drugs employed in this study were carmustine (BCNU Nitrumon, Sintesa S.A., Bruxelles, Belgium), indinavir sulfate (IDV, Sigma-Aldrich, Milan, Italy), phlorizin (PHZ, Sigma-Aldrich), ritonavir (RTV, Sigma-Aldrich), and temozolomide (TMZ, Sigma-Aldrich). BCNU was resuspended in absolute ethanol; IDV in pure water; PHZ, RTV, and TMZ in DMSO (Sigma-Aldrich) and used at the indicated concentrations. Aphidicolin (Sigma-Aldrich) was used to treat U87MG cells at 1-μM concentration for 24 hours to block cell growth. Antibodies employed and dilutions were the following: anti-actin (1:5000, cat. A4700 Sigma-Aldrich), anti-AMPKα F6 (1:2000, cat. 2793 Cell Signaling Technology, Danvers, MA), anti–phospho-AMPKα Thr172 40H9 (1:1000, cat. 2535 Cell Signaling Technology), anti-GLUT1/SLC2A1 (1:10,000, cat. 07-1401 Merck-Millipore, Vimodrone, MI, Italy), anti– Golgin-97 CDF4 (1:3000, cat. A-21270, Thermo Fisher Scientific, Waltham, MA), anti-GFP (1:700, chicken polyclonal, Aves Labs, Tigard, OR). Species-specific secondary antibodies labeled with peroxidase (Thermo Fisher Scientific) or with Alexa Fluor 488 (1:500, Jackson ImmunoResearch, West Grove, PA) were employed, respectively, for Western blot or immunohistochemistry.

### Protein Extraction and Western Blot

For protein immunoblot analysis, cells were harvested and lysed in ice-cold RIPA buffer (150 mM NaCl, 50 mM Tris-HCl pH 8.0, 1% TritonX-100, 0.1% sodium deoxycholate, 0.1% sodium dodecyl sulfate, 1 mM $Na_2VO_4$) supplemented with 1× "Complete Mini Proteases Inhibitor Cocktail" (Roche, Monza, Italy). Protein samples were quantified by Qubit fluorometer (Thermo Fisher Scientific) following manufacturer's instructions. One hundred fifty micrograms of protein extract was loaded per lane. Antibody binding was detected by the "ECL Select Western Blotting Detection Kit" (GE Healthcare, Milan, Italy).

### Cell Proliferation and Glucose Consumption

Growth of U87MG, Hu197, GBM-P1, and GL261 cells was tested after plating $5 × 10^5$ cells per well in six-well plate. The cells were treated with the drug of interest or the combination of drugs, and cell counts were performed after 24 hours. For growth curve

experiments, $2 \times 10^5$ cells per well were plated, and counting was performed every 24 hours from the beginning of the treatment on at least three wells. Cells were counted on a Z2 Beckman Coulter counter (Beckman Coulter, Cassina De' Pecchi, MI, Italy); before counting, cells in multicellular tumor spheroids (MTS) were first disaggregated by trypsin.

Glucose uptake in cell cultures was evaluated at the appropriate times by sampling 300 µl of medium from the plate where the cells were growing. After centrifugation (2000$g$) to remove floating cells and cell debris, glucose was measured by a potentiometric method on an automatic blood gas analyzer (ABL800 Flex, Radiometer, Milan, Italy) certified for clinical use.

### Construction of the Isobolograms

To distinguish synergy from additivity or antagonism of the combination of one glucose transport inhibitor with BCNU or TMZ, we constructed, for each combination, a specific isobologram. Isobolograms were plotted by evaluating the concentration of two interacting drugs giving the same effect on cell growth [25]. The inhibiting concentration 50 (IC50) value is defined as the drug concentration reducing by 50% the growth of treated cells compared with control ones. We determined the IC50 of each drug separately by plating either U87MG or GL261 cells and adding TMZ, BCNU, RTV, IDV, or PHZ at several drug concentrations spanning their probable range of activity. After 24 hours of treatment, the cells were counted as described before. Each IC50 value was graphically derived and then verified experimentally. Combination index (CI) was defined as follows: $CI = [C]_{A50}/IC50_A + [C]_{B50}/IC50_B$, where $[C]_{A50}$ and $[C]_{B50}$ are the concentrations in combination inducing the given effect. A CI of less than, equal to, or more than 1 indicates, respectively, synergy, additivity, or antagonism.

Growth-inhibitory activity of the drug combinations BCNU/RTV, TMZ/RTV, and BCNU/IDV was measured by counting the cells after 24 hours of treatment in six-well plates and comparing the values to the number of control cells: only the combinations giving the same inhibitory effect of the IC50 were plotted on the isobologram graphs. The line of additivity was constructed by interpolating the two points corresponding to the IC50 of the two drugs. Graphically, synergy, additivity, and antagonism are indicated by a point plotted below, on, or above the line of additivity.

### Low-Density Microvesicles Isolation

Glucose transporters are membrane-bound proteins, and their function depends on the composition of lipids in the external or inner membranes where they reside [26]. For this reason, GLUT/SLC2A concentration in the cytosol is low. To increase GLUT1/SLC2A1 concentration, we purified a membrane fraction enriched in membranes from low-density vesicles in the cells [27]. Briefly, U87MG cells were harvested after the appropriate treatment and resuspended in the homogenization medium (0.25 M sucrose, 1 mM EDTA, 20 mM Hepes-NaOH, pH 7.4). The cells were homogenized in a 7-ml glass Dounce homogenizer, and after centrifugation for 10 minutes at 1000 rpm, the pellet containing the nuclear fraction was discarded. The supernatants were further centrifuged for 20 minutes at 14000 rpm, and the secondary pellet containing organelles and high-density microvesicles was discarded. Supernatants were finally centrifuged for 30 minutes at 44,000 rpm to isolate the final pellet containing the purified low-density microvesicles (LDMs). LDMs were then lysed by RIPA buffer and subjected to Western blot analysis as described before.

### Animal Experiments

Briefly, twenty-four 2- to 3-month-old female C57BlC mice were stereotactically implanted under deep general anesthesia (isoflurane supplemented with nitrous oxide) with $1 \times 10^5$ GL261 glioblastoma cells. The cells were stereotactically inoculated through a burr hole by a Hamilton syringe into the left striatum (coordinates: 1 mm anteroposterior and 1 mm lateral from bregma, at a depth of 3 mm). All experimental procedures were conducted in accordance with the European Communities Council Directive of 24 November 1986 (86/609 EEC), Recommendation 18/06/2007, Dir. 2010/63/UE, and the Italian law for care and use of experimental animals (DL116/92) and were approved by the Italian Ministry of Health (prot. E669C.15) and the Bioethical Committee of the University of Turin. All animals were housed under a 12-hour light:dark cycle in an environmentally controlled room. All experiments were designed to minimize the numbers of animals used and their discomfort. In each experiment, animals with tumors were allocated to one of four groups: no treatment (controls), BCNU alone (2.5 mg/kg), combination of RTV (100 mg/kg) and BCNU (1.5 mg/kg), or combination of RTV (100 mg/kg) and BCNU (2.5 mg/kg). RTV was administered every day up to the death of the animal. All drugs were administered intraperitoneally, and treatments were started 10 days after tumor implantation. Animals that were transplanted with GL261 cells expressing eGFP were euthanized after the second magnetic resonance imaging (MRI) scan. Briefly, they were transcardially perfused under deep anesthesia (ketamine 100 mg/mg, Ketavet, Bayern, Leverkusen, Germany; xylazine 5 mg/kg, Rompun, Bayern, Leverkusen, Germany) with 4% paraformaldehyde in 0.12 M phosphate buffer, pH 7.2 to 7.4. The brains were dissected and cut in 50 µm–thick cryostat coronal sections. Sections were incubated overnight at room temperature with a polyclonal anti-GFP antibody dissolved in PBS with 1.5% donkey serum (Jackson ImmunoResearch) and 0.25% Triton X-100 (Sigma Aldrich) and then exposed for 2 hours at room temperature to secondary species-specific antibody. The nuclei were counterstained with 4′,6-diamidino-2-phenylindole. After processing, sections were mounted on microscope slides with Tris-glycerol supplemented with 10% Mowiol (Calbiochem). Analysis of images obtained from histological sections was performed with the open-source Java image processing program ImageJ 1.50i [28].

### MRI Experiments

MRI experiments were randomly performed on two animals in each group to monitor tumor growth. The selected animals were imaged 8 to 10 days post–cell inoculation and 14 days after the beginning of the treatment. MRI were acquired at 7.1 T using a Bruker Avance 300 spectrometer equipped with a Micro 2.5 imaging probe and a birdcage resonator with an inner diameter of 30 mm. The breath rate was constantly monitored throughout *in vivo* MRI experiments using a respiratory probe (SAII Instruments, Stony Brook, NY). Before MRI, mice were anesthetized by injecting a mixture of tiletamine/zolazepam (Zoletil 100; Virbac, Milan, Italy) 20 mg/kg and xylazine (Rompun; Bayer, Milan, Italy) 5 mg/kg. Intravenous administration of the clinically approved contrast agent MultiHance (gadobenate dimeglumine, Bracco Diagnostics, Italy) at 0.5 mmol/kg was performed to provide T1 contrast. After the scout image acquisition, both T2-weighted (T2w) and T1-weighted (T1w) images were acquired to precisely locate the tumor. T2w high-resolution anatomical images were acquired with a Turbo-Rare

sequence (repetition time = 2500 milliseconds; echo time = 36 milliseconds; rare factor = 8; slice thickness = 1 mm; 9 slices; field of view = 3 cm; matrix = 384 × 384; number of averages = 5; total imaging time = 10 minutes). T1w multislice multiecho images were acquired 15 minutes post–Multihance injection with the same geometry of T2w high-resolution images (repetition time = 250 milliseconds; echo time = 4.65 milliseconds; matrix = 256 × 256; number of averages = 10; total imaging time = 10 minutes and 40 seconds). Both T2w and T1w images were acquired with coronal geometry.

MR data analysis was carried out with Bruker Paravision 5.1 Software. The tumor area was delineated in each slice in both T2w and T1w images by manually drawing regions of interest along tumor borders. The 3D tumor volume was then assessed by summing up volumes obtained through multiplication of each region of interest for the slice thickness.

### Statistical Analysis

Statistical significance was assessed by parametric (unpaired Student's *t* test) and nonparametric (Mann-Whitney test) methods. Survival was calculated by using the date each mouse was found dead or moribund. Survival curves were obtained by Kaplan-Meier analysis, and significant differences in survival were evaluated by the log-rank test by using MedCalc software, version 16.8.84.

## Results

### RTV, IDV, and PHZ Differentially Affect Human and Murine GBM Cell Proliferation

We determined the IC50 value of RTV, IDV, and PHZ on cell proliferation by counting the number of cells in adherent cultures of human U87MG or murine GL261 glioblastoma cells after 24 hours of exposure to increasing concentrations of each drug separately. The IC50 of RTV was 45 μM for U87MG and 55 μM for GL261. The IC50 of IDV for U87MG was 500 μM and higher than 500 μM for GL261. We could not determine the IC50 concentration of PHZ because even at concentrations close to its maximum solubility in DMSO (100 mM), it induced less than 50% of cell growth inhibition in both cell lines (Figure 1*A*). At the tested concentrations of RTV, IDV, and PHZ, the cells cultures did not show signs of increased cytotoxicity, suggesting that, at least in the first 24 hours of treatment, these drugs inhibited cell proliferation without inducing cell death. After we established the IC50s of RTV and IDV in U87MG, we tested in the same cell line if the inhibition of cell growth was stable at longer times. The growth curves generated in the presence of the previously determined IC50 concentrations of RTV or IDV or the maximal PHZ concentration we used before showed that the growth-inhibitory effects were maintained up to 72 hours (Figure 1, *B-G*). By comparing the growth curves obtained with the different drugs, we found that RTV induced more stable and prolonged growth inhibition of U87MG cells. We also found that the same concentration of RTV used for U87MG and GL261 cells also inhibited growth of Hu197, an unrelated human glioblastoma cell line, and of primary human glioblastoma cells maintained in the absence of serum (Figure 1, *A* and *E*). MTS formed *in vitro* by the aggregation of glioblastoma cells are considered a better *in vitro* model of the metabolic conditions found in glioblastoma *in vivo*, and they allow better preservation of hallmark molecular alterations of cancer than monolayer cultures [24,29]. We also tested on MTS derived

from U87MG cells if the same concentration of RTV was inhibitory of cell growth, and we found that, in the presence of RTV (45 μM), MTS were fewer and smaller compared with controls (Figure 2). Growth curves obtained by counting glioblastoma cells after dissociation of MTS confirmed the growth-inhibitory effect of RTV. The results of the above experiments indicate that RTV and IDV but not PHZ inhibit glioblastoma cell growth. However, RTV is more powerful than IDV, and 10 times more IDV on a molar basis are required to equal the inhibition obtained by RTV.

### Inhibition of Glioblastoma Cell Growth by RTV, IDV, and PHZ Is Proportional to the Inhibition of Glucose Uptake

We measured the uptake of glucose and the activation of aerobic glycolysis in U87MG glioblastoma cells maintained in the presence or absence of RTV, IDV, and PHZ by monitoring the levels of glucose and lactate in the cell medium. We found that levels of inhibition of glucose uptake and lactate production were proportional to the inhibitory effect on cell growth of each drug; PHZ had no effect on glucose consumption. Similar results were obtained when glucose consumption and lactate production were evaluated after blocking cell division in all culture conditions by the addition of aphidicolin, an inhibitor of B-family of DNA polymerases [30]. Treating all cultures both under control and experimental conditions with aphidicolin resulted in a complete stop of cell growth; thus, differences in cell number did not interfere with the measurements of glucose uptake. Even in the presence of aphidicolin, RTV was the best inhibitor of glucose consumption (Figure 3, *A-C*).

Glucose starvation has a profound influence on glioblastoma cell metabolism resulting, among other effects, in a rapid increase in intracellular AMP enhancing its binding to the γ subunit of the AMPKα. After AMP binding, AMPKα undergoes an allosteric transition that increases phosphorylation on Thr172 by serine/threonine kinase 11. To confirm the biological significance of the reduction in glucose uptake induced in U87MG cells by drug treatments, we compared the level of AMPKα activation by phosphorylation on Thr172 induced by the complete exhaustion of glucose in the culture media with the effects induced by RTV or IDV treatment (Figure 3, *D* and *E*). We found that phosphorylation of AMPKα increased in glioblastoma cells treated by RTV at levels comparable with those of the same cells growing in the absence of glucose, whereas in IDV-treated cells, it did not change significantly compared with controls (Figure 3, *D* and *E*).

### RTV But Not IDV Acts Synergically with BCNU or TMZ in Inhibiting Glioblastoma Cell Growth In Vitro

We then assessed if the addition of BCNU or TMZ to RTV and IDV could enhance its cytostatic effect on glioblastoma cells. We performed an isobologram analysis of the combination of RTV or IDV with BCNU or TMZ (Figure 4, *A-C*). As a preliminary step for the analysis, we determined experimentally the IC50 dose of BCNU and TMZ that in U87MG and GL261 cell cultures resulted, respectively, 50 μM and 40 μM for BCNU and 400 μM for TMZ. These values are in good agreement with the values reported in the literature [31]. The isobolograms for U87MG and GL261 cells obtained by the simultaneous exposure of the cells to RTV and BCNU or RTV and TMZ demonstrated, at all concentrations tested, a clear synergism of the drug combinations. Conversely, we only obtained indications of additivity or even antagonism when the same cells were exposed to IDV and BCNU. Table 1 reports the
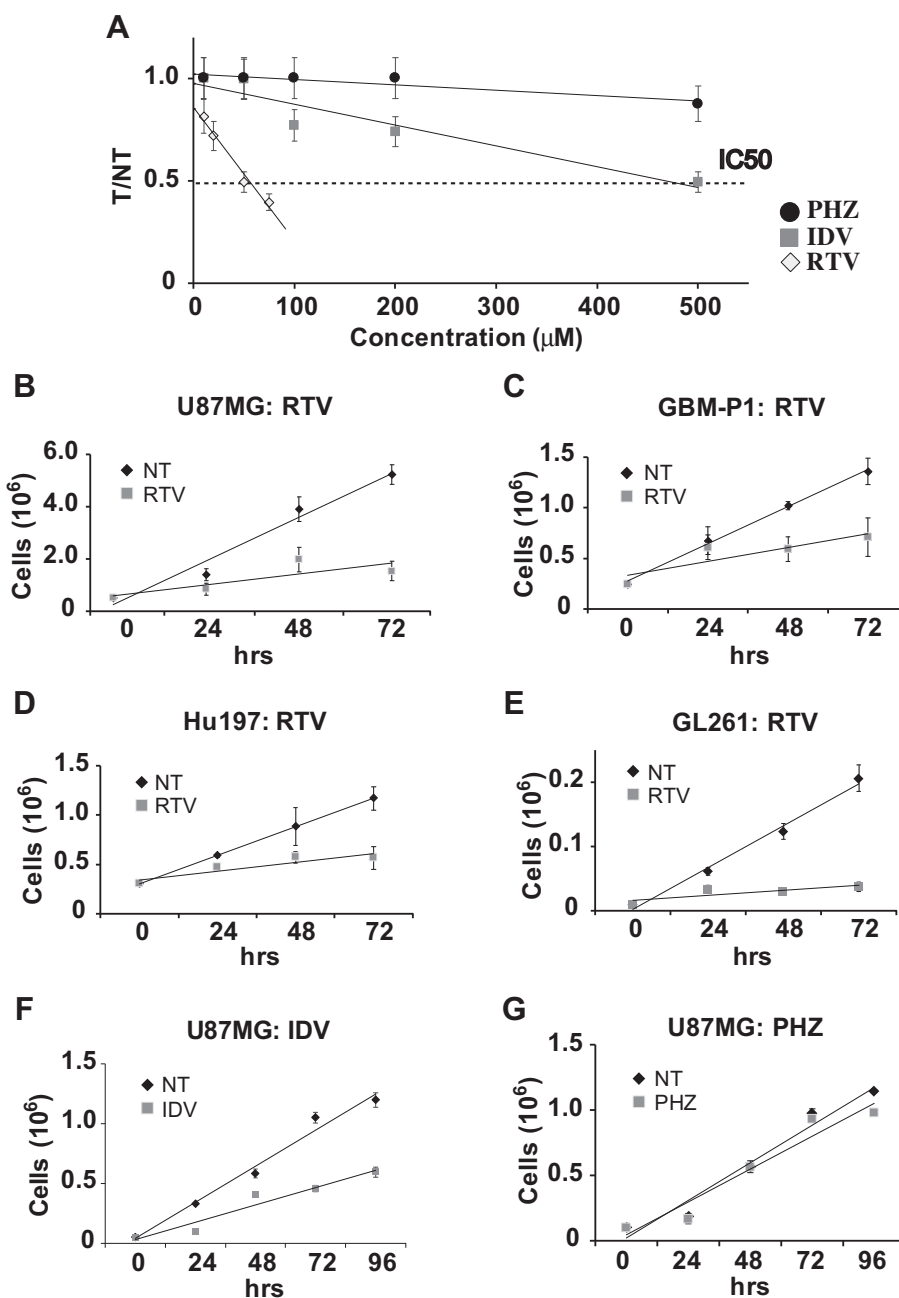
**Figure 1.** *In vitro* effects of RTV, IDV, and PHZ on glioblastoma cells. (A) IC50 values determined for IDV, PHZ, and RTV in U87MG cells. IC50 represents the drug concentration reducing by 50% the growth of treated cells compared with control ones. The IC50 of RTV was 45 $\mu$M, approximately 10 times lower than the IC50 of IDV (500 $\mu$M). We were unable to determine the IC50 of PHZ because PHZ never induced 50% inhibition compared with control cells even at the maximal concentration we could dissolve PHZ in DMSO (100 mM). *Y*-axis (T/NT) represents the mean value of the ratio between the number of the cells in the wells (at least 3) with the addition of the drug (T) and the number of the cells in the control wells (NT) (at least 3). (B-G) Growth curves derived from RTV treatment of the human U87MG glioblastoma cell line (B), GBM-P1 primary human glioblastoma-derived cells (C), human glioblastoma Hu197 cell line (D), and mouse glioblastoma GL261 cell line (E). Growth response of U87MG glioblastoma cell line to the addition of IDV (F) or PHZ (G) was also tested *in vitro*. The growth was followed up to 72 hours. RTV and IDV were used at the IC50 concentration we previously determined for each cell type, whereas PHZ was used at the maximal concentration we tested before. For RTV, IC50 was 45 $\mu$M for U87MG, GBM-P1, and Hu197 and 55 $\mu$M for mouse GL261 cells. RTV induced consistent growth inhibition in all glioblastoma cell cultures. Error bars depict standard deviation.

combinations of concentrations used in the isobolograms and the calculated CIs. In U87MG, the stronger synergism between BCNU and RTV was obtained with the ratios of 1:0.7 (20 $\mu$M:13 $\mu$M) and 1:2.5 (10 $\mu$M:22 $\mu$M) and the similar CI of 0.7. Comparable CIs

values (0.7) were also obtained for the TMZ-RTV combination. We obtained similar results when we tested the different drug combinations on GL261 cells with a CI of 0.7 for the BCNU-RTV combination that is the same obtained in U87MG cells.
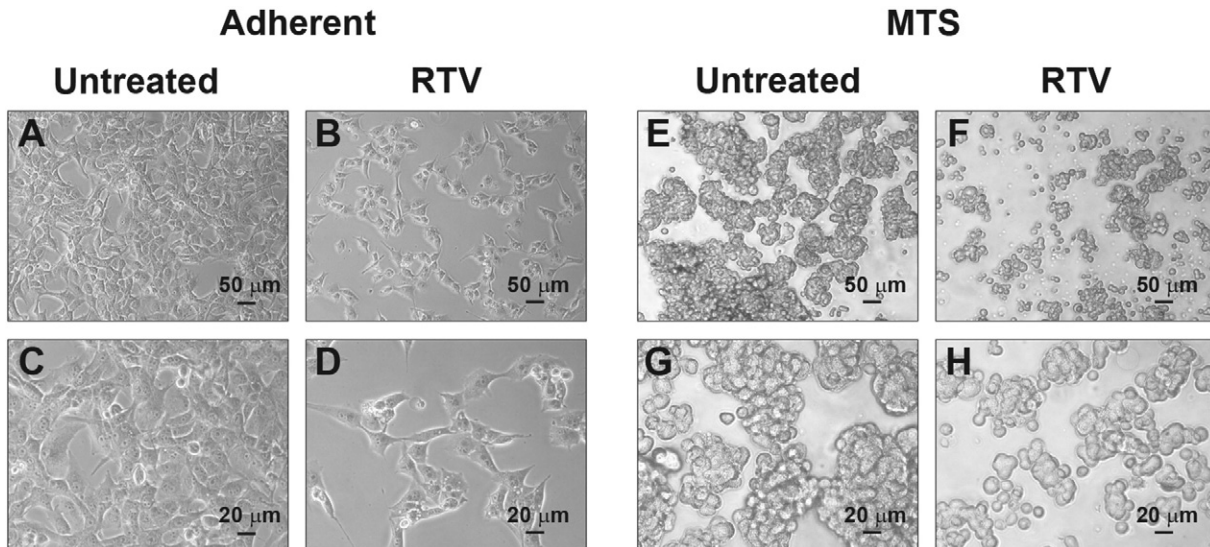
**Figure 2.** Microphotographs of U87MG cells growing in adherence (A-D) or in MTS (E-H), control conditions (A, C, E, and G), or after addition of RTV (45 $\mu$M) (B, D, F, and H). After RTV treatment, cell proliferation is reduced as shown by the reduction both in the number of adherent cells (B, D) and in the size and abundance of MTS (F, H). Scale bars are in $\mu$m.
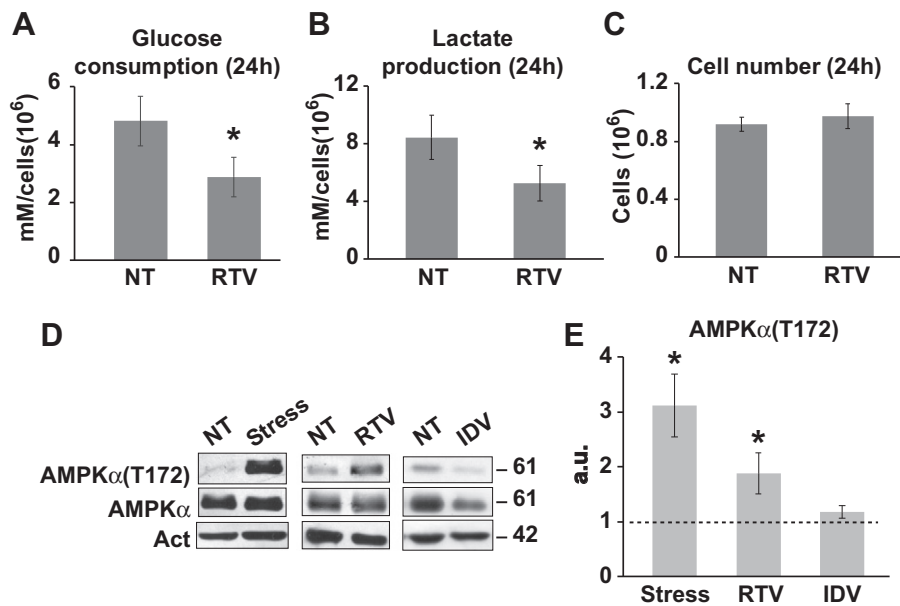


**Figure 3.** Twenty-four–hour treatment of RTV inhibits glucose consumption and lactate production in U87MG cells. After RTV treatment, we measured the concentration of glucose (A) and lactate (B) in the medium, and we observed a significant decrease in glucose uptake and lactate production; this reduction indicates a significant inhibition of glycolysis. As RTV treatment reduces cell proliferation, we performed the experiment in the presence of aphidicolin at a concentration blocking cell division (1 $\mu$M) to maintain a comparable number of cells in untreated (NT) and RTV-treated (RTV) cultures (C). Histograms derived from two independent experiments; at least three wells per experiment. Asterisk indicates values from controls ($P < .05$ unpaired $t$ test). Error bars indicate standard deviation. (D) Western blot analysis: AMPKα activation was demonstrated in U87MG cells by an increase in the level of threonine (T172) phosphorylation compared with control; AMPKα was activated by metabolic stress (Stress) or RTV (45 $\mu$M) treatment; IDV (500 $\mu$M) treatment did not induce AMPKα activation. Act: immunoreactivity for actin. On the right, the corresponding molecular weights are indicated (kDa). (E) Histogram representing the results of the densitometric analysis of Western blot bands of three independent experiments confirming that AMPKα activation is significantly induced by Stress or RTV but not by IDV. "a.u." (arbitrary units) indicates differences in AMPK activation in stressed (Stress), RTV- or IDV-treated *versus* untreated cells. Asterisks indicate $P < .05$ compared with NT sample. Error bars indicate standard deviation.
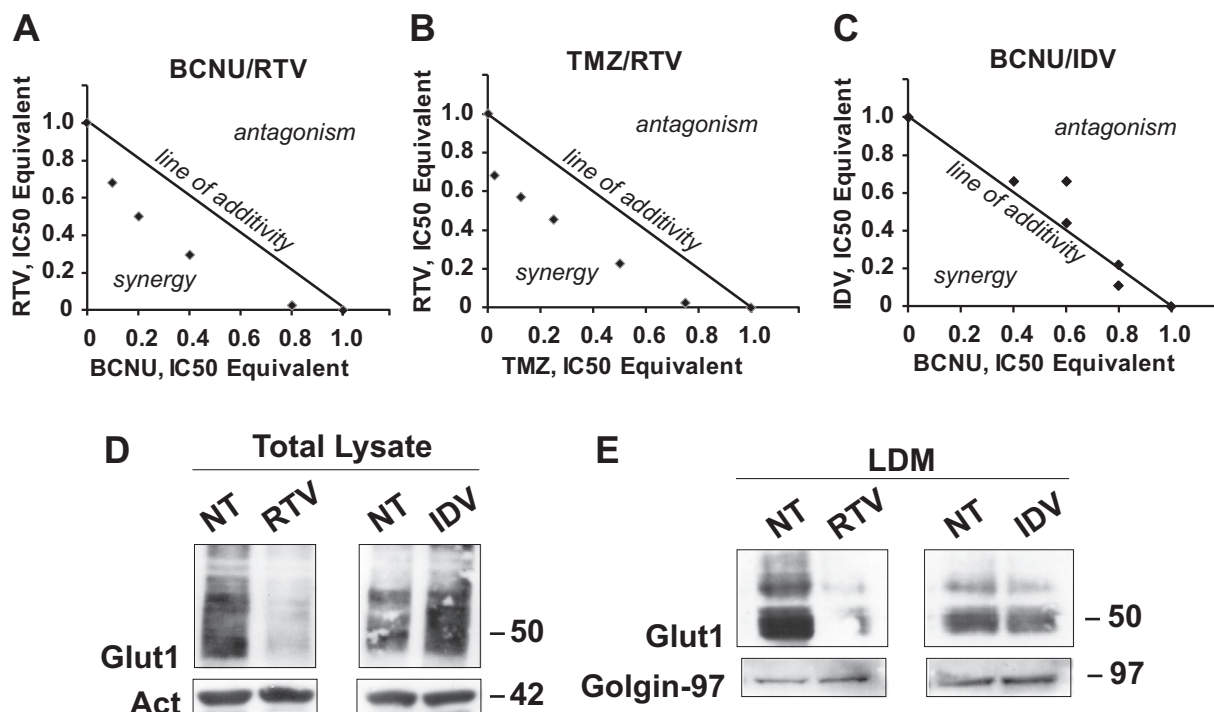
**Figure 4.** (A) Isobolograms analysis of inhibition of growth of U87MG cells (A-C) and effects of RTV and IDV treatment on GLUT1/SLC2A1 transporter levels in U87MG cells (D-E). (A-C) The "line of additivity" connects the values of the IC50 of the two drugs used in combination, thus separating the quadrant into two parts; points plotted below the line of additivity indicate synergy (activity of the combination is larger than expected for the simple combination of the two drugs), whereas points above the line indicate antagonism (activity of the combination is lower than the expected for the simple combination of the two drugs). BCNU-RTV: (A) The two drugs at all tested concentrations show synergic activity. TMZ-RTV: (B) The two drugs at all tested concentrations show synergic activity. BCNU-IDV: (C) The two drugs show addictive or antagonistic behavior at all concentrations except for the highest, when we obtained an indication of minimal synergic activity. (D) Western blot of total lysates of U87MG cells: RTV reduced the level of GLUT1/SLC2A1 immunoreactivity, whereas IDV increased GLUT1/SLC2A1 level compared with untreated cells (NT). The same membrane was stripped and reacted with an antibody against actin (Act) whose level was similar in all samples. (E) As in D, but the cells were fractionated, and only the fraction containing the LDMs, where the GLUTs-containing vesicles reside, was analyzed by Western blot. As in the total extract, the GLUT1/SLC2A1 signal was decreased only by RTV treatment. The same membrane was stripped and reacted with an antibody against Golgin-97 whose level was similar in all samples. Numbers indicate the molecular weights in kDa.

### IDV But Not RTV Induces a Compensatory Increase in GLUT1/SLC2A1

IDV is a more powerful and specific inhibitor of GLUT4/SLC2A4 and has little or no inhibitory activity on GLUT1/SLC2A1 and GLUT3/SLC2A3, whereas RTV is less efficient than IDV in inhibiting GLUT4/SLC2A4 (Figure 4D). However, because of its broader specificity, RTV inhibits the activity of multiple members of the GLUT/SLC2A superfamily [18,19]. Because multiple members of the GLUT/SLC2A superfamily are expressed in glioblastoma cells, we hypothesized that strong inhibition of GLUT4/SLC2A4 activity by IDV could result in upregulation of other members of the superfamily to compensate for the reduced uptake of glucose. We purified the LDM fraction from U87MG cells after 24 hours of RTV (45 μM) or IDV (500 μM) treatment and from untreated cells. The LDM fraction is enriched in vesicles and cell membranes containing members of the GLUT/SLC2A superfamily. We analyzed the LDM fractions from the different treatment conditions by Western blot using a monoclonal antibody against GLUT1/SLC2A1, and we found that RTV treatment decreased the level of GLUT1/SLC2A1, whereas IDV did not reduce but slightly increased the level of GLUT1/SLC2A1 compared with untreated cells (Figure 4E).

### RTV Acts Synergically with BCNU in Inhibiting Glioblastoma Cell Growth In Vivo

We generated glioblastoma in mice brain by stereotactically injecting $1 \times 10^5$ GL261 cells into the left striatum of adult mice. Tumor formation was evaluated in randomly chosen mice by contrast MRI 10 days after inoculation of the cells. Mice where then divided into four groups I) control, II) mice receiving BCNU (2.5 mg/kg, i.p.), III) mice receiving both BCNU (1 mg/kg, i.p.) the first day and RTV (100 mg/kg, i.p.) every day up to death or sacrifice of the animal, and IV) mice receiving both BCNU (2.5 mg/kg, i.p.) the first day and RTV (100 mg/kg, i.p.) every day up to death or sacrifice of the animal. Animals receiving BCNU alone or in combination that were still surviving 27 days after tumor inoculation received a second i.p. injection of BCNU at the same concentration used for the first. Animals initially submitted to MRI were rescanned 2 weeks after the first examination (Figure 5). Mice receiving an inoculum of GL261 cells expressing eGFP were euthanized after the second MRI and processed for histology to confirm the neoplastic nature of the alterations seen in the MRI (Figure 6A). The MRI scans demonstrated that the average tumor volume in mm³ of control mice was 39.33 (S.D. ±38.88), of mice treated by 2.5 mg/kg BCNU

**Table 1.** Combination Index Analysis

| BCNU (μM) | RTV (μM) | BCNU IC50EQ | RTV IC50EQ | Ratio | CI CI = (d1/50) + (d2/45) | |
|---|---|---|---|---|---|---|
| 50 | 0 | 1.0000 | 0.0000 | | | |
| 40 | 1 | 0.8000 | 0.0227 | 1:0.03 | 0.82 | Synergy |
| 20 | 13 | 0.4000 | 0.2955 | 1:0.7 | 0.70 | Synergy |
| 10 | 22 | 0.2000 | 0.5000 | 1:2.5 | 0.70 | Synergy |
| 5 | 30 | 0.1000 | 0.6818 | 1:6.8 | 0.88 | Synergy |
| 0 | 45 | 0.0000 | 1.0000 | | | |

| TMZ (μM) | RTV (μM) | TMZ IC50EQ | RTV IC50EQ | Ratio | CI CI = (d1/400) + (d2/45) | |
|---|---|---|---|---|---|---|
| 400 | 0 | 1.0000 | 0.0000 | | | |
| 300 | 1 | 0.7500 | 0.0227 | 1:0.003 | 0.77 | Synergy |
| 200 | 10 | 0.5000 | 0.2273 | 1:0.05 | 0.73 | Synergy |
| 100 | 20 | 0.2500 | 0.4545 | 1:0.2 | 0.70 | Synergy |
| 50 | 25 | 0.1250 | 0.5682 | 1:0.5 | 0.69 | Synergy |
| 10 | 30 | 0.0250 | 0.6818 | 1:3 | 0.71 | Synergy |
| 0 | 45 | 0.0000 | 1.0000 | | | |

| BCNU (μM) | IDV (μM) | BCNU IC50EQ | IDV IC50EQ | Ratio | CI CI = (d1/50) + (d2/500) | |
|---|---|---|---|---|---|---|
| 50 | 0 | 1.0000 | 0.0000 | | | |
| 40 | 50 | 0.8000 | 0.1100 | 1:1.25 | 0.91 | Synergy |
| 40 | 100 | 0.8000 | 0.2200 | 1:2.50 | 1.02 | Additivity |
| 30 | 200 | 0.6000 | 0.4400 | 1:6.67 | 1.04 | Additivity |
| 30 | 300 | 0.6000 | 0.6600 | 1:10 | 1.26 | Antagonism |
| 20 | 300 | 0.4000 | 0.6600 | 1:15 | 1.06 | Additivity |
| 0 | 500 | 0.0000 | 1.0000 | | | |

was 91 (S.D. ±123.04), of mice treated by 1 mg/kg BCNU and 100 mg/kg RTV was 27 (S.D. ± 20.53), and of mice treated by 2.5 mg/kg BCNU and 100 mg/kg RTV was 20 (S.D. ±15.67). Although a trend associating a reduction of tumor volume with the addition of RTV to BCNU is apparent, it did not reach statistical

significance. However, the Kaplan-Meier survival analysis showed a significant statistical difference in overall survival for mice treated by RTV and BCNU compared with control mice or mice treated by BCNU alone ($\chi^2$ 11.74, degrees of freedom 3, $P$ = .0083) (Figure 6$B$). Interestingly, both tumor volume and overall survival of mice receiving BCNU and RTV were not significantly different in mice treated with 1 mg/kg compared with 2.5 mg/kg of BCNU.

## Discussion

Highly efficient glucose uptake through glucose transporters is important for brain tumor initiating cell growth and survival in glioblastoma [32]. Increased glucose uptake is instrumental in maintaining an enhanced glycolic activity that is essential for survival of the mesenchymal subtype of glioblastoma [33]. Furthermore, long-term treatment of glioblastoma cells with TMZ, the most common chemotherapeutic agent used in the adjuvant treatment of GBM, upregulates expression of GLUT/SLC2A family members [34]. Inhibition of glucose uptake and/or aerobic glycolysis are thus considered potentially important targets for glioblastoma therapy [35]. We exploited the off-target inhibitory effects of RTV on GLUT1/SLC2A1, GLUT4/SLC2A4, and other members of the GLUT/SLC2A superfamily to inhibit the growth of human and murine glioblastoma cells both *in vitro* and *in vivo*. Our results demonstrated that the growth-inhibitory effect of RTV treatment on human and murine glioblastoma cells parallels its effects on glucose uptake as predicted from its inhibition of multiple glucose transporters of the GLUT/SLC2A superfamily [18,19]. On the contrary, IDV, another HIV protease inhibitor, whose off-target effects are limited to GLUT4/SLC2A4 [17], resulted to be less active in inhibiting glioblastoma cell growth. However, both RTV and IDV reach cerebrospinal fluid concentrations *in vivo* that are less than one order of magnitude of their plasma concentration [36]. Interestingly, others, after having considered the potential proteasomal inhibitory activity of RTV, unsuccessfully attempted to inhibit *in vivo* the growth of a 9L rat gliosarcoma tumor model by administering RTV as a single agent [37]. On the contrary, RTV is active *in vitro* as a single
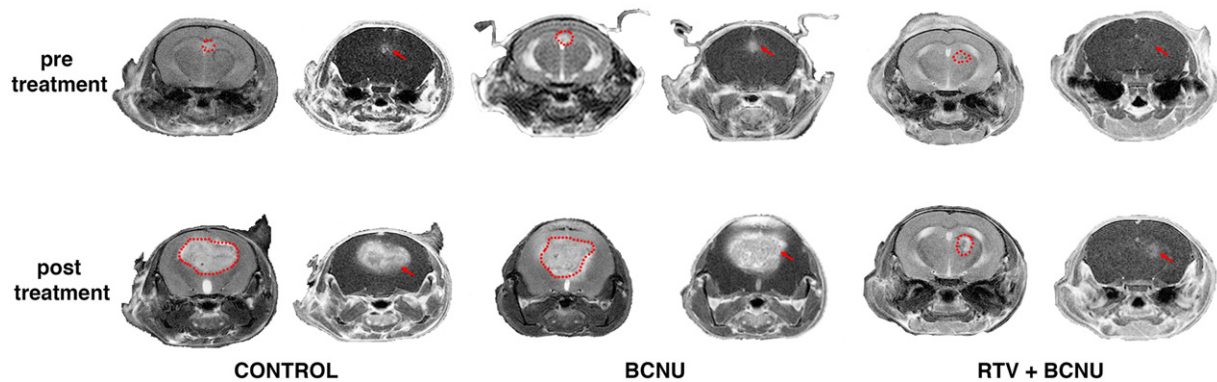


**Figure 5.** The effect of BCNU alone and BCNU + RTV on tumor growth *in vivo*. Mice were inoculated with GL261 cells and imaged after 10 days just before the start of treatment, and 14 days later. The images are divided into three groups according to treatments: control (CTRL), BCNU (BCNU 1.5 mg/kg alone), BCNU (same as before). and RTV (100 mg/kg). In each group, the first row (pretreatment) shows the results of MRIs performed on day 10 after tumor inoculation, whereas the second row (post treatment) shows images obtained 14 days after the start of treatment (24 days after the inoculum). For each animal, in the first column, T2-weighted images are reported, whereas in the second column, T1-weighted images after gadolinium injection are displayed. The stippled lines present in T2-weighted images delimit the area of the tumor, whereas the tumor is indicated by an arrow in the corresponding T1-weighted images.
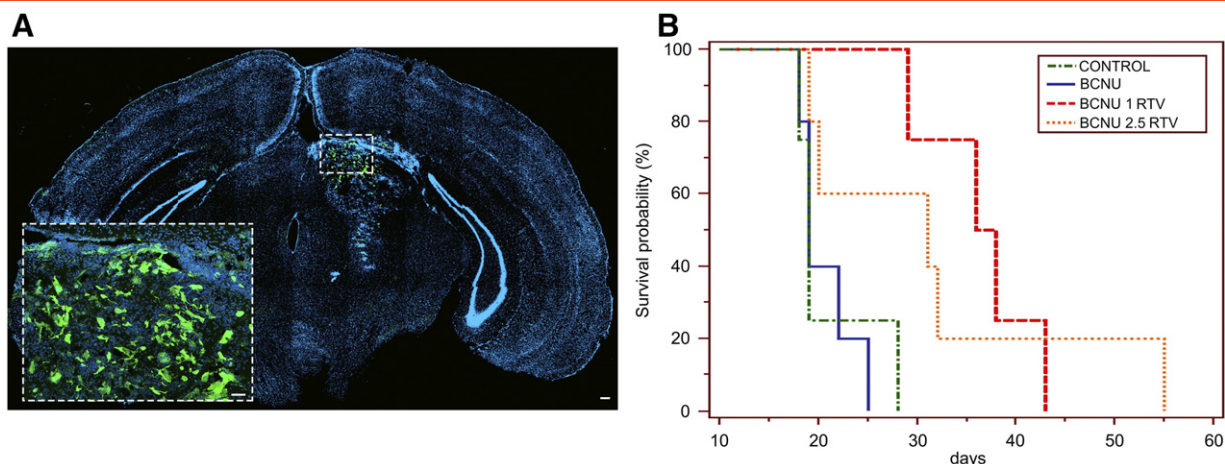
**Figure 6.** (A) eGFP-expressing GL261 glioma cells grow and infiltrate the host brain 2 weeks after the initial inoculum; control animal. Microphotograph showing a coronal section of the tumor-bearing brain. Cell nuclei are stained by 4′,6-diamidino-2-phenylindole. GL261 cells fluoresce in green. EGFP-positive GL261 glioma cells spread into the left striatum and adjacent structures, occupying 4.9% of the brain hemispheres. The area boxed is shown at higher magnification in the inset. Scale bars: 30 $\mu$M in A and 10 $\mu$M in the inset. (B) Kaplan-Meier analysis of survival of mice bearing GL261 gliomas treated by BCNU alone or BCNU and different amounts of RTV as indicated in the box. Each treatment group of mice is indicated by a different line texture and color. Control mice, inoculated with GL261 cells and left untreated, are indicated in green. Mice inoculated with GL261 cells and injected i.p. 12 days after with BCNU (2.5 mg/kg) are indicated in orange. Mice inoculated with GL261 cells and injected i.p. 12 days after with BCNU (2.5 mg/kg) and RTV (100 mg/kg) are indicated in red. After the initial administration, BCNU was administered every 2 weeks, whereas RTV i.p. injections were repeated daily up to the death of the mice. Comparison of survival curves (log-rank test) showed a significant effect of the addition of RTV on survival compared with controls and BCNU alone ($\chi^2$: 12.7816; degrees of freedom 3; $P = .0051$).

agent or in combination with TMZ against gliosarcoma and high-grade glioma cells [37,38]. The results of our isobologram analysis of the combined effects of RTV and BCNU or TMZ on human and murine glioblastoma cells revealed that RTV *in vitro* does synergize the growth-inhibitory effects of both chemotherapeutic agents, whereas IDV when used in combination with BCNU is, at its best, only additive. These results suggest that multiple glucose transporter inhibition is necessary for the synergic effect of RTV with BCNU or TMZ. We preferred to test *in vivo* the combination of RTV with BCNU because TMZ treatment upregulates expression of GLUT/SLC2A family members [34], therefore possibly interfering with RTV action at the low doses achievable in the cerebrospinal fluid. Furthermore, hematologic, hepatic, and pulmonary cumulative dose-limiting toxicity is worse with BCNU compared with TMZ [2]. The possibility of obtaining a similar antiglioblastoma response with single-dose reduction by combining BCNU with RTV is thus more relevant clinically for BCNU, which could in principle be administered for longer times before reaching its cumulative limiting dose. The results of the *in vivo* experiments show that RTV (100 mg/kg) synergizes the growth-inhibitory action of BCNU, prolonging mice survival even at doses of BCNU as low as 1 mg/kg that are at least five times lower than the lower dose commonly administered to mice for brain tumor therapy [39] and just two times the dose administered, without apparent toxicity, to reduce the amyloid plaque burden in an Alzheimer's mouse model [40]. The dose of RTV we employed *in vivo* is the dose employed as single agent against the rat 9L gliosarcoma model that failed to give any indication of prolonged survival [37]. However, the results of our isobologram analysis on glioblastoma cells suggest that, when used in combination with BCNU, the dose of RTV could be reduced to minimize the negative effects of chronic RTV administration like insulin resistance, dyslipidemia, and lipodystrophy [41]. Interestingly, the

current clinical indication for RTV is as a pharmacokinetic enhancer of other HIV protease inhibitors, predominantly due to its inhibitory effect on P-glycoprotein and the cytochrome P450 3A4 isoenzyme [42]. This effect could also enhance *in vivo* the activity of BCNU against high-grade gliomas, allowing further modulation of the dose. In conclusion, our findings support the idea that RTV, despite its poor penetration of the blood-brain barrier, synergizes with BCNU *in vitro* and *in vivo*, allowing a significant decrease in the level of BCNU necessary to control the growth of GBM. Considering that both and BCNU are already approved and their side effects well known, a clinical study on high-grade glioma patients based on drug repositioning of RTV in combination with BCNU or TMZ seems interesting.

## Conflict of Interest Statement

The authors declare that there is no conflict of interest in this work.

## References

[1] Stupp R, Brada M, Van Den Bent MJ, Tonn JC, Pentheroudakis G, and ESMO Guidelines Working Group (2014). High-grade glioma: ESMO Clinical Practice Guidelines for diagnosis, treatment and follow-up. *Ann Oncol* **25**(Suppl. 3), iii93–ii101. http://dx.doi.org/10.1093/annonc/mdu050.

[2] Bay JO, Linassier C, Biron P, Durando X, Verrelle P, Kwiatkowski F, Rosti G, Demirer T, and EMBT solid tumors working party (2007). Does high-dose carmustine increase overall survival in supratentorial high-grade malignant glioma? An EBMT retrospective study. *Int J Cancer* **120**, 1782–1786. http://dx.doi.org/10.1002/ijc.223035.

[3] Aronin PA, Jr Mahaley MS, Rudnick SA, Dudka L, Donohue JF, Selker RG, and Moore P (1980). Prediction of BCNU pulmonary toxicity in patients with malignant gliomas: an assessment of risk factors. *N Engl J Med* **303**, 183–188. http://dx.doi.org/10.1056/NEJM198007243030403.

[4] Huang TT, Hudson MM, Stokes DC, Krasin MJ, Spunt SL, and Ness KK (2011). Pulmonary outcomes in survivors of childhood cancer: a systematic review. *Chest* **140**, 881–901. http://dx.doi.org/10.1378/chest.10-2133.

[5] Girgin F, Tüzün S, Demir A, Kuralay F, Ozutemiz O, and Tanyalcin T (1999). Cytoprotective effects of trimetazidine in carmustine cholestasis. *Exp Toxicol Pathol* **51**, 326–329.

[6] Chang SM, Prados MD, Yung WK, Fine H, Junck L, Greenberg H, Robins HI, Mehta M, Fink KL, Jaeckle KA, et al (2004). Phase II study of neoadjuvant 1, 3-bis (2-chloroethyl)-1-nitrosourea and temozolomide for newly diagnosed anaplastic glioma: a North American Brain Tumor Consortium Trial. *Cancer* **100**, 1712–1716. http://dx.doi.org/10.1002/cncr.20157.

[7] Gutenberg A, Bock HC, Brück W, Doerner L, Mehdorn HM, Roggendorf W, Westphal M, Felsberg J, Reifenberger G, and Giese A (2013). MGMT promoter methylation status and prognosis of patients with primary or recurrent glioblastoma treated with carmustine wafers. *Br J Neurosurg* **27**, 772–778. http://dx.doi.org/10.3109/02688697.2013.791664.

[8] Mohrenz IV, Antonietti P, Pusch S, Capper D, Balss J, Voigt S, Weissert S, Mukrowsky A, Frank J, Senft C, et al (2013). Isocitrate dehydrogenase 1 mutant R132H sensitizes glioma cells to BCNU-induced oxidative stress and cell death. *Apoptosis* **18**, 1416–1425. http://dx.doi.org/10.1007/s10495-013-0877-8.

[9] Tomicic MT, Aasland D, Nikolova T, Kaina B, and Christmann M (2013). Human three prime exonuclease TREX1 is induced by genotoxic stress and involved in protection of glioma and melanoma cells to anticancer drugs. *Biochim Biophys Acta* **1833**, 1832–1843. http://dx.doi.org/10.1016/j.bbamcr.2013.03.029.

[10] Reithmeier T, Graf E, Piroth T, Trippel M, Pinsker MO, and Nikkhah G (2010). BCNU for recurrent glioblastoma multiforme: efficacy, toxicity and prognostic factors. *BMC Cancer* **10**, 30. http://dx.doi.org/10.1186/1471-2407-10-30.

[11] Nishioka T, Oda Y, Seino Y, Yamamoto T, Inagaki N, Yano H, Imura H, Shigemoto R, and Kikuchi H (1992). Distribution of the glucose transporters in human brain tumors. *Cancer Res* **52**, 3972–3979.

[12] Nagamatsu S, Sawa H, Wakizaka A, and Hoshino T (1993). Expression of facilitative glucose transporter isoforms in human brain tumors. *J Neurochem* **61**, 2048–2053.

[13] Labak CM, Wang PY, Arora R, Guda MR, Asuthkar S, Tsung AJ, and Velpula KK (2016). Glucose transport: meeting the metabolic demands of cancer, and applications in glioblastoma treatment. *Am J Cancer Res* **6**, 1599–1608.

[14] Uhlén M, Fagerberg L, Hallström BM, Lindskog C, Oksvold P, Mardinoglu A, Sivertsson A, Kampf C, Sjostedt E, Asplund A, et al (2015). Proteomics. Tissue-based map of the human proteome. *Science* **347**, 1260419. http://dx.doi.org/10.1126/science.1260419.

[15] Strowd RE, Cervenka MC, Henry BJ, Kossoff EH, Hartman AL, and Blakeley JO (2015). Glycemic modulation in neuro-oncology: experience and future directions using a modified Atkins diet for high-grade brain tumors. *Neurooncol Pract* **2**, 127–136. http://dx.doi.org/10.1093/nop/npv010.

[16] Rieger J, Bähr O, Maurer GD, Hattingen E, Franz K, Brucker D, Walenta S, Kammerer U, Coy JF, Weller M, et al (2014). ERGO: a pilot study of ketogenic diet in recurrent glioblastoma. *Int J Oncol* **44**, 1843–1852. http://dx.doi.org/10.3892/ijo.2014.2382 [Erratum in: Int J Oncol. **45** (2014) 2605].

[17] Murata H, Hruz PW, and Mueckler M (2000). The mechanism of insulin resistance caused by HIV protease inhibitor therapy. *J Biol Chem* **275**, 20251–20254. http://dx.doi.org/10.1074/jbc.C000228200.

[18] Hresko RC and Hruz PW (2011). HIV protease inhibitors act as competitive inhibitors of the cytoplasmic glucose binding site of GLUTs with differing affinities for GLUT1 and GLUT4. *PLoS One* **6**e25237. http://dx.doi.org/10.1371/journal.pone.0025237.

[19] Hresko RC, Kraft TE, Tzekov A, Wildman SA, and Hruz PW (2014). Isoform-selective inhibition of facilitative glucose transporters: elucidation of the molecular mechanism of HIV protease inhibitor binding. *J Biol Chem* **289**, 16100–16113. http://dx.doi.org/10.1074/jbc.M113.528430.

[20] Szatmári T, Lumniczky K, Désaknai S, Trajcevski S, Hídvégi EJ, Hamada H, and Safrany G (2006). Detailed characterization of the mouse glioma 261 tumor model for experimental glioblastoma therapy. *Cancer Sci* **97**, 546–553. http://dx.doi.org/10.1111/j.1349-7006.2006.00208.x.

[21] Ponten J and Macintyre EH (1968). Long term culture of normal and neoplastic human glia. *Acta Pathol Microbiol Scand* **74**, 465–486. http://dx.doi.org/10.1111/j.1699-0463.1968.tb03502.x.

[22] Allen M, Bjerke M, Edlund H, Nelander S, and Westermark B (2016). Origin of the U87MG glioma cell line: Good news and bad news. *Sci Transl Med* **8**, 354re3. http://dx.doi.org/10.1126/scitranslmed.aaf6853.

[23] Gerosa MA, Talarico D, Fognani C, Raimondi E, Colombatti M, Tridente G, De Carli L, and Della Valle G (1989). Overexpression of N-ras oncogene and epidermal growth factor receptor gene in human glioblastomas. *J Natl Cancer Inst* **81**, 63–67.

[24] Azzalin A, Moretti E, Arbustini E, and Magrassi L (2014). Cell density modulates SHC3 expression and survival of human glioblastoma cells through Fak activation. *J Neuro-Oncol* **120**, 245–256. http://dx.doi.org/10.1007/s11060-014-1551-x.

[25] Zhao L, Au JL, and Wientjes MG (2010). Comparison of methods for evaluating drug-drug interaction. *Front Biosci (Elite Ed)* **2**, 241–249.

[26] Hresko RC, Kraft TE, Quigley A, Carpenter EP, and Hruz PW (2016). Mammalian Glucose Transporter Activity Is Dependent upon Anionic and Conical Phospholipids. *J Biol Chem* **291**, 17271–17282. http://dx.doi.org/10.1074/jbc.M116.730168.

[27] Yeh TY, Sbodio JI, Tsun ZY, Luo B, and Chi NW (2007). Insulin-stimulated exocytosis of GLUT4 is enhanced by IRAP and its partner tankyrase. *Biochem J* **402**, 279–290. http://dx.doi.org/10.1042/BJ20060793.

[28] Schneider CA, Rasband WS, and Eliceiri KW (2012). NIH Image to ImageJ: 25 years of image analysis. *Nat Methods* **9**, 671–675.

[29] Wittig R, Richter V, Wittig-Blaich S, Weber P, Strauss WS, Bruns T, Dick TP, and Schneckenburger H (2013). Biosensor-expressing spheroid cultures for imaging of drug-induced effects in three dimensions. *J Biomol Screen* **18**, 736–743. http://dx.doi.org/10.1177/1087057113480525.

[30] Baranovskiy AG, Babayeva ND, Suwa Y, Gu J, Pavlov YI, and Tahirov TH (2014). Structural basis for inhibition of DNA replication by aphidicolin. *Nucleic Acids Res* **42**, 14013–14021. http://dx.doi.org/10.1093/nar/gku1209.

[31] Mihaliak AM, Gilbert CA, Li L, Daou MC, Mose RP, Reeves A, Cochran BH, and Ross AH (2010). Clinically relevant doses of chemotherapy agents reversibly block formation of glioblastoma neurospheres. *Cancer Lett* **296**, 168–177. http://dx.doi.org/10.1016/j.canlet.2010.04.005.

[32] Flavahan WA, Wu Q, Hitomi M, Rahim N, Kim Y, Sloan AE, Weil RJ, Nakano I, Sarkaria JN, Stringer BW, et al (2013). Brain tumor initiating cells adapt to restricted nutrition through preferential glucose uptake. *Nat Neurosci* **16**, 1373–1382. http://dx.doi.org/10.1038/nn.3510.

[33] Mao P, Joshi K, Li J, Kim SH, Li P, Santana-Santos L, Luthra S, Chandran UR, Benos PV, Smith L, et al (2013). Mesenchymal glioma stem cells are maintained by activated glycolytic metabolism involving aldehyde dehydrogenase 1A3. *Proc Natl Acad Sci U S A* **110**, 8644–8649. http://dx.doi.org/10.1073/pnas.1221478110.

[34] Le Calvé B, Rynkowski M, Le Mercier M, Bruyère C, Lonez C, Gras T, Haibe-Kains B, Bontempi G, Decaestecker C, Ruysschaert JM, et al (2010). Long-term in vitro treatment of human glioblastoma cells with temozolomide increases resistance in vivo through up-regulation of GLUT transporter and aldo-keto reductase enzyme AKR1C expression. *Neoplasia* **12**, 727–739 [Erratum in: Neoplasia, **13** (2011) 5p following 886].

[35] Purow B (2016). For glioma, a sweet side to diabetes. *Neuro Oncol* **18**, 306–307. http://dx.doi.org/10.1093/neuonc/nov328.

[36] Ene L, Duiculescu D, and Ruta SM (2011). How much do antiretroviral drugs penetrate into the central nervous system? *J Med Life* **4**, 432–439.

[37] Laurent N, de Boüard S, Guillamo JS, Christov C, Zini R, Jouault H, Andre P, Looteau V, and Peschanski M (2004). Effects of the proteasome inhibitor ritonavir on glioma growth in vitro and in vivo. *Mol Cancer Ther* **3**, 129–136.

[38] Kast RE, Ramiro S, Lladó S, Toro S, Coveñas R, and Muñoz M (2016). Antitumor action of temozolomide, ritonavir and aprepitant against human glioma cells. *J Neuro-Oncol* **126**, 425–431. http://dx.doi.org/10.1007/s11060-015-1996-6.

[39] Leuraud P, Taillandier L, Medioni J, Aguirre-Cruz L, Crinière E, Marie Y, Kujas M, Golmard JL, Duprez A, Delattre JY, et al (2004). Distinct responses of xenografted gliomas to different alkylating agents are related to histology and genetic alterations. *Cancer Res* **64**, 4648–4653. http://dx.doi.org/10.1158/0008-5472.CAN-03-3429.

[40] Hayes CD, Dey D, Palavicini JP, Wang H, Patkar KA, Minond D, Nefzi A, and Lakshmana MK (2013). Striking reduction of amyloid plaque burden in an Alzheimer's mouse model after chronic administration of carmustine. *BMC Med* **11**, 81. http://dx.doi.org/10.1186/1741-7015-11-81.

[41] Vyas AK, Koster JC, Tzekov A, and Hruz PW (2010). Effects of the HIV protease inhibitor ritonavir on GLUT4 knock-out mice. *J Biol Chem* **285**, 36395–36400. http://dx.doi.org/10.1074/jbc.M110.176321.

[42] Renjifo B, van Wyk J, Salem AH, Bow D, Ng J, and Norton M (2015). Pharmacokinetic enhancement in HIV antiretroviral therapy: a comparison of ritonavir and cobicistat. *AIDS Rev* **17**, 37–46.